

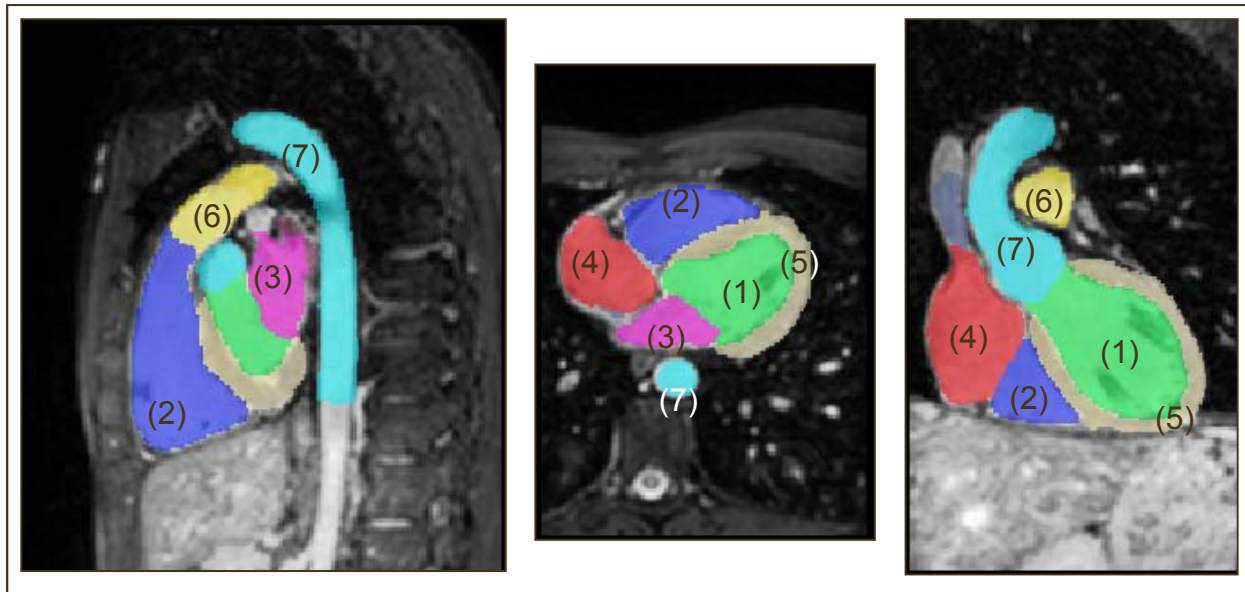
A Registration-Based Atlas Propagation Framework for Automatic Whole Heart Segmentation

Xiahai Zhuang (PhD)

Centre for Medical Image Computing
University College London

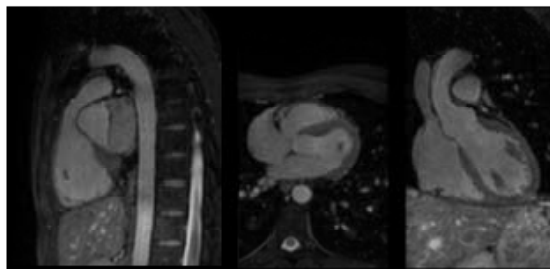
- Whole heart segmentation and challenges
- Whole heart segmentation framework
 - LARM: Locally Affine Registration Method
- Experiments and results
- Conclusion and extension works

- Whole heart segmentation
 - Ventricle (myocardium)
 - Atria
 - And sometimes great vessels if needed

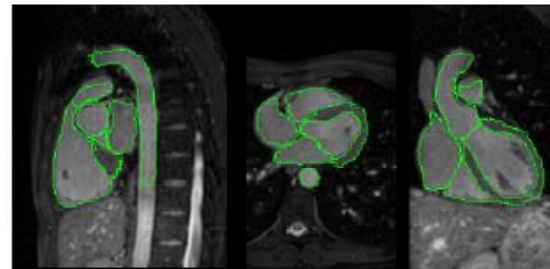


Left ventricle (1), right ventricle (2), left atrium (3), right atrium (4), myocardium (5), pulmonary artery (6), and aorta (7).

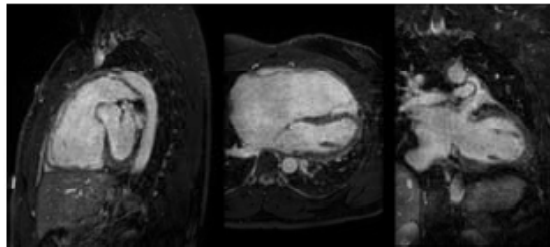
- Challenges of automation:
 - **Large shape variability**
 - Indistinct boundaries
 - Noise, artefacts, intensity inhomogeneity



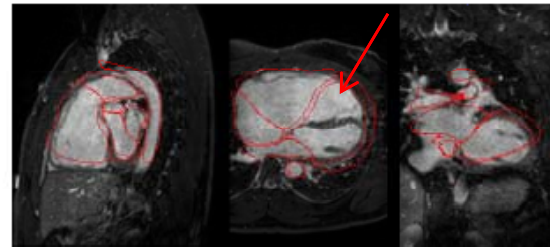
(a)



(b)



(c)



(d)

- (a) MR image from a healthy volunteer; (b) a successful segmentation of (a) using a model based segmentation ;
(c) MR image from a patient with right ventricle hypertrophy; (d) an erroneous segmentation of (c).

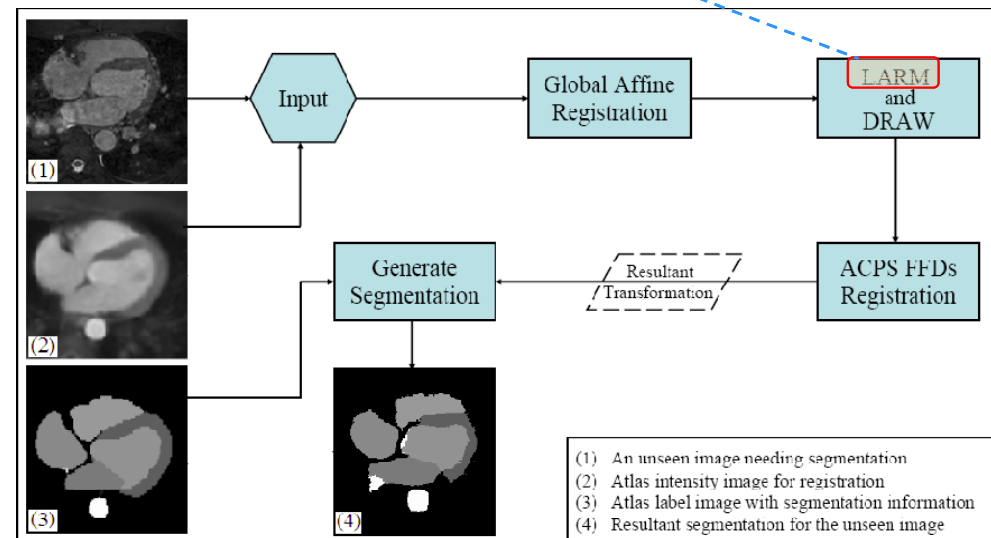
- Atlas propagation using image registration

Zhuang, X., *et al.*: An atlas-based segmentation propagation framework using locally affine registration -Application to automatic whole heart segmentation. *MICCAI* 2008

Zhuang, X., *et al.*: Free-Form Deformations Using Adaptive Control Point Status for Whole Heart MR Segmentation. *Functional Imaging and Modelling of the Heart* 2009

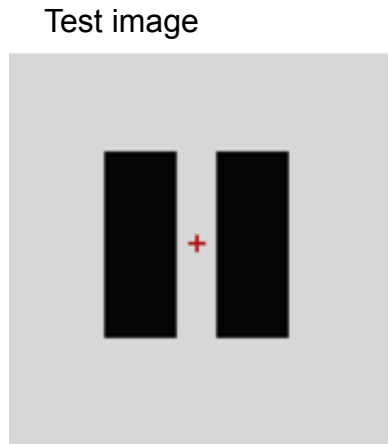
Zhuang, X., *et al.*: A Registration-Based Propagation Framework for Automatic Whole Heart Segmentation of Cardiac MRI. *IEEE Trans. Med. Imag.* 29 (9), 1612-1625, 2010.

LARM: locally affine registration method

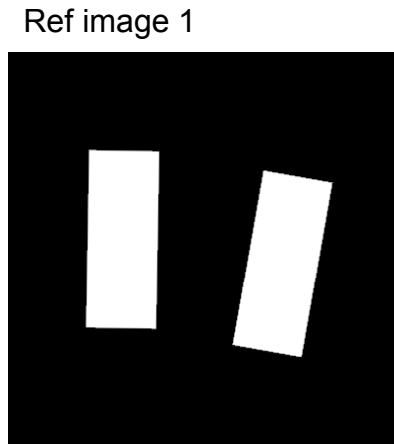


Shape from **an** atlas + LARM = model the variations for all cardiac images with different shapes

1. Difference intensity distribution (modality)



(a)



(b)

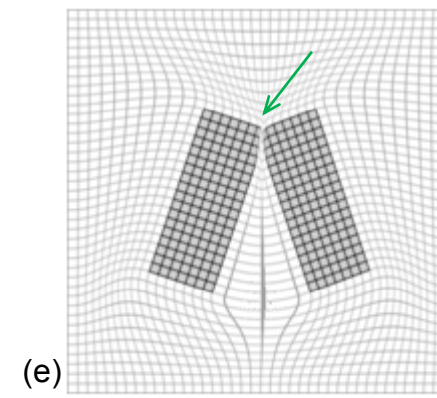
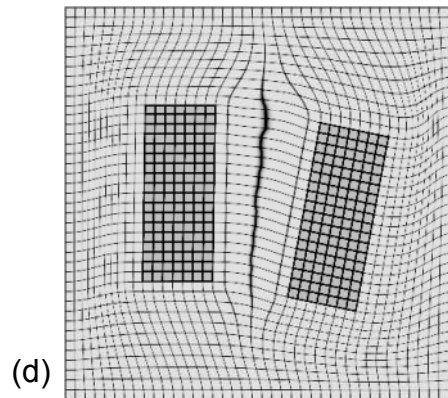


(c)

Locally affine transformation model:

- 1) Pre-defined local regions
- 2) Assign an affine for each local region

Registration result: transformation field



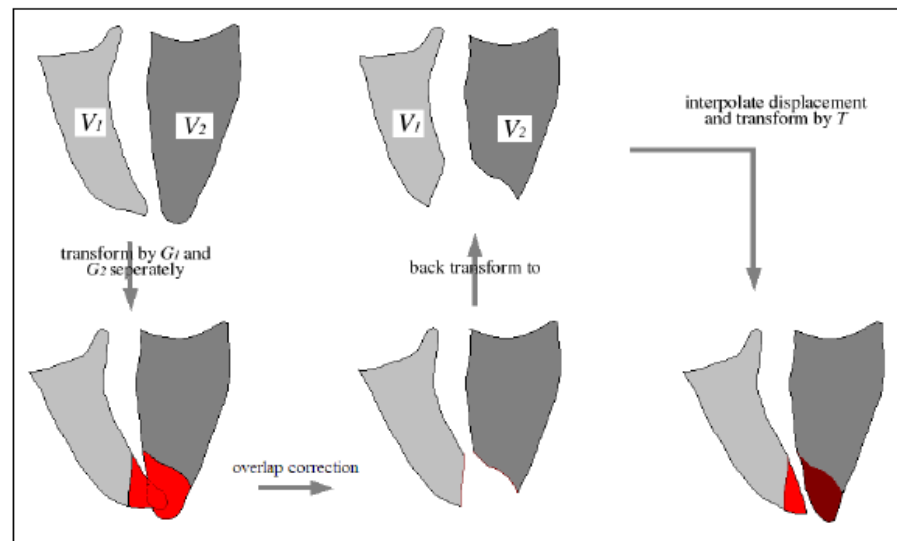
2. Locally: preserve the affinity or maximally preserve the affinity
3. Globally: maintain diffeomorphic mapping

- Locally affine transformation model

$$T(X) = \begin{cases} G_i(X), & X \in U_i, i=1\dots n \\ \sum_{i=1}^n w_i(X)G_i(X_i), & X \notin \bigcup_{i=1}^n U_i \end{cases} \quad w_i(X) = (1/d_i(X)^e) / \left(\sum_{i=1}^n 1/d_i(X)^e \right)$$

Where $\{U_i\}$ and $\{G_i\}$ are local regions and assigned affine transformations and $\{w_i\}$ are normalized weighting functions, $d_i(X)$ is distance between X and U_i .

1. Region overlap -> correction $V_i = G_i^{-1}(G_i(V_i) - \mathbf{DI}_L(R_{ij}))$



- Locally affine transformation model
 1. Region overlap
 2. **Folding caused by large displacements**

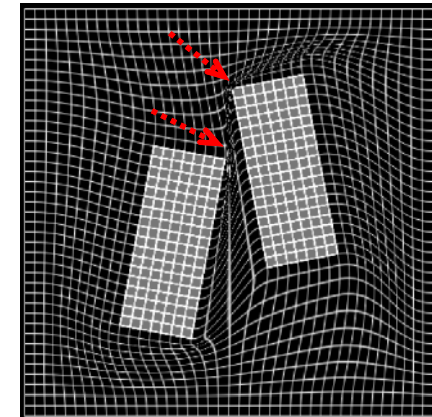
-> Monitor Jacobian matrix

and concatenation

- Jacobian matrix:

$$J_T = \sum_{i=1}^n \frac{\partial w_i}{\partial x} G_i + \sum_{i=1}^n w_i \frac{\partial G_i}{\partial x} = \nabla \mathbf{W} \cdot \mathbf{G}^T + \nabla \mathbf{G} \cdot \mathbf{W}^T$$

- Monitor the determinant: $\|J(T_c)\| < 0.5$
- Whenever the condition is met, we apply current locally affine transformation result T_c to the source/target image to generate a new one, and then reset the registration
- Final transformation is the concatenation of each locally affine transformations: $T = T_1 \circ T_2 \circ \dots \circ T_m$



- Similarity measure

- Mutual information

$$\begin{aligned}
 MI(I_r, I_f) &= H(I_r) + H(I_f) - H(I_r, I_f) \\
 H(I_r, I_f) &= - \sum_{r, f} p(r, f) \log p(r, f) \\
 p(i) &= \sum_{x \in \Omega} \omega(I(x))
 \end{aligned} \tag{1}$$

I : image intensity; H : entropy;

p : probability function; ω is parzen window function.

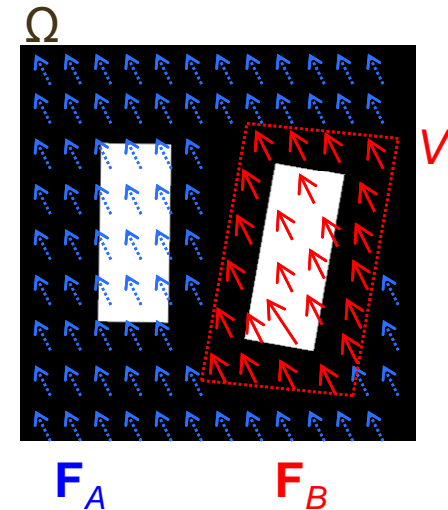
- Computation of driving forces

$$F_{\theta_i} := \frac{\partial H}{\partial \theta_i} = \left(- \sum_p (1 + \log(p)) \frac{\partial P_A}{\partial \theta_i} \right) + \left(- \sum_p (1 + \log(p)) \frac{\partial P_B}{\partial \theta_i} \right) = F_A + F_B \tag{2}$$

$$p = P_A + P_B \quad P_A = \sum_{x \in \bar{V}_i} \omega(I(x)) \quad P_B = \sum_{x \in V_i} \omega(I(x))$$

$$\longrightarrow F_{\theta_i} := F_B = - \sum_p (1 + \log(p)) \cdot \frac{\partial P_B}{\partial \theta_i} \tag{3}$$

Save up to 100 times computation time in the 3D cardiac application without losing registration accuracy



- Similarity measure

- Mutual information

$$\begin{aligned} MI(I_r, I_f) &= H(I_r) + H(I_f) - H(I_r, I_f) \\ H(I_r, I_f) &= - \sum_{r,f} p(r, f) \log p(r, f) \end{aligned} \quad (1)$$

$$p(i) = \sum_{x \in \Omega} \omega(I(x)) \quad \text{global intensity from } \Omega$$

- Computation of driving forces

$$F_{\theta_i} := \frac{\partial H}{\partial \theta_i} = \left(- \sum_p (1 + \log(p)) \frac{\partial P_A}{\partial \theta_i} \right) + \left(- \sum_p (1 + \log(p)) \frac{\partial P_B}{\partial \theta_i} \right) = F_A + F_B \quad (2)$$

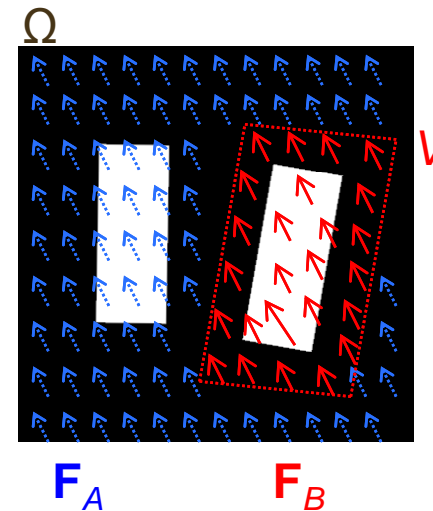
$$p = P_A + P_B \quad P_A = \sum_{x \in \bar{V}_i} \omega(I(x)) \quad P_B = \sum_{x \in V_i} \omega(I(x))$$

$$\longrightarrow F_{\theta_i} := F_B = - \sum_p (1 + \log(p)) \cdot \frac{\partial P_B}{\partial \theta_i} \quad (3)$$

- Different from region-based registration [Zhuang, et al. SPIE'08]

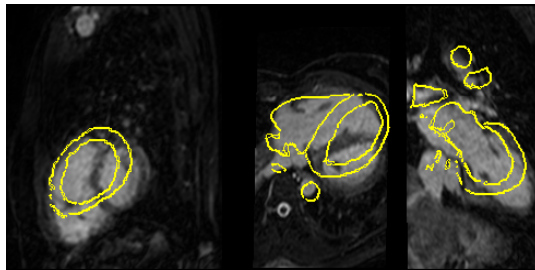
- Each local region is extracted and registered to the target image separately

$$F_{\theta_i} = - \sum_p (1 + \log(P_B)) \cdot \frac{\partial P_B}{\partial \theta_i} \quad (4) \quad \text{local intensity from } V$$

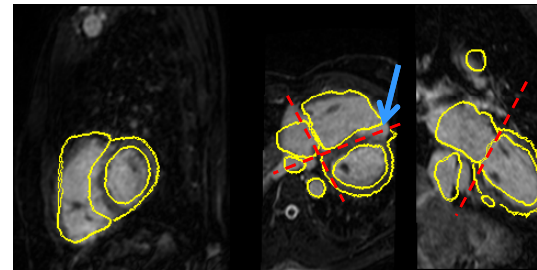


[Zhuang, et al.: In: SPIE Vol. 6914 Medical Imaging 2008: Image Processing, 6914, 07, 2008.]

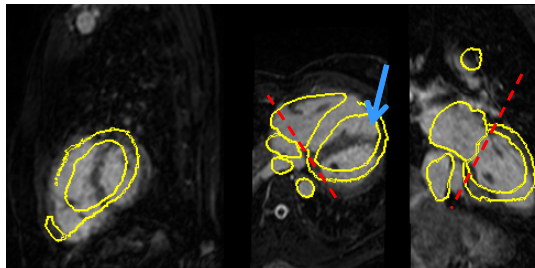
- Applied to whole heart segmentation for initialisation
 - Hierarchy scheme



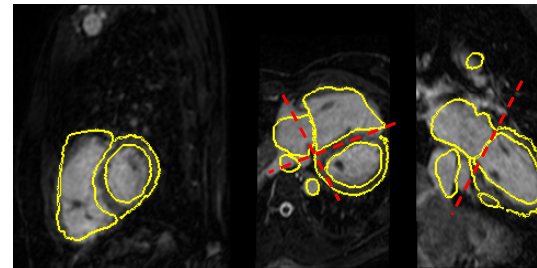
1) After global affine registration



3) After LARM of four regions

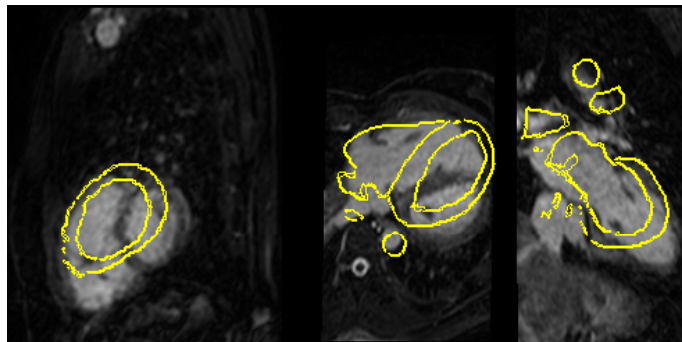


2) After LARM of two regions



4) After LARM of seven regions

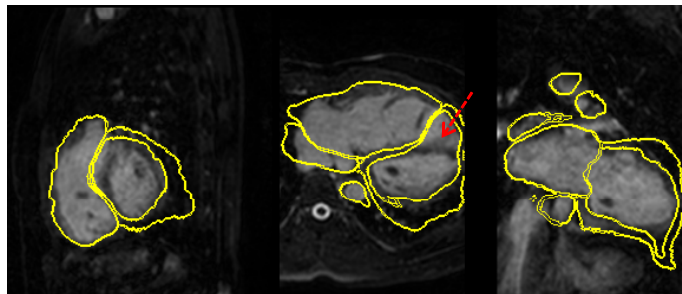
Bad initialization by **global affine registration**



(a)

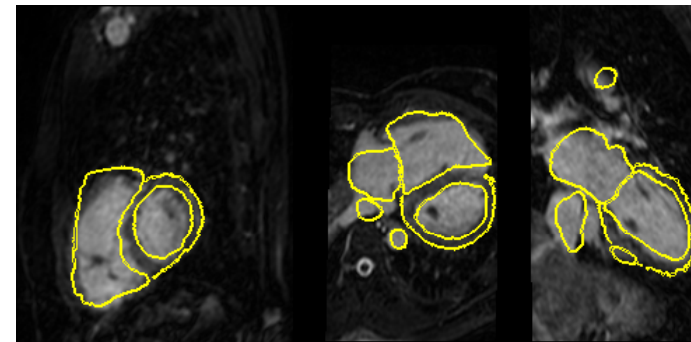


FFD nonrigid propagation result using global affine registration for initialization



(c)

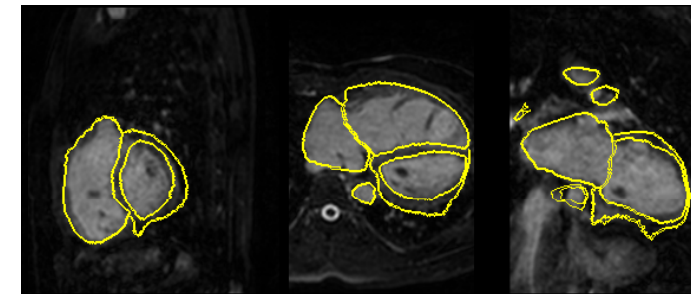
Good initialization by **locally affine registration method**



(b)



FFD nonrigid propagation result using locally affine registration for initialization



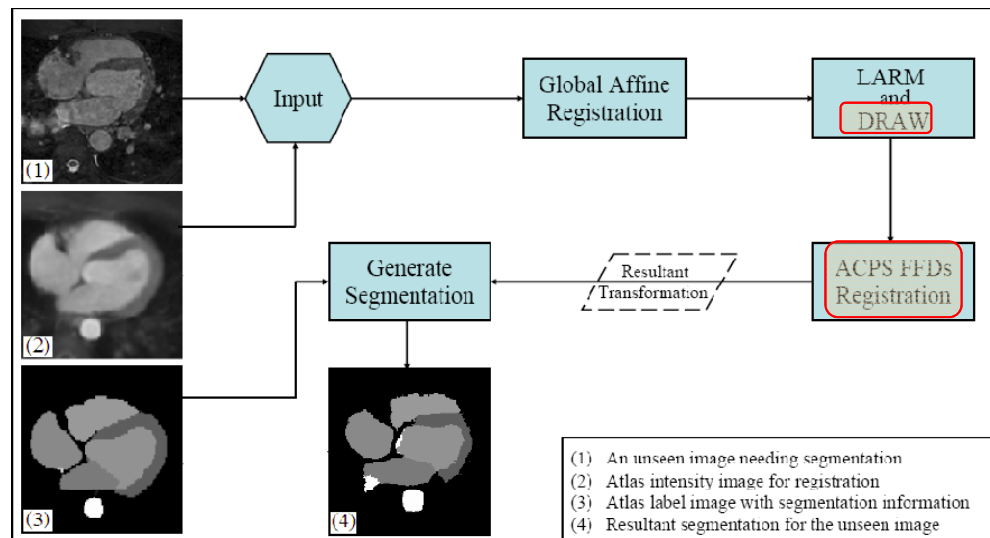
(d)

- Atlas propagation using image registration

Zhuang, X., *et al.*: An atlas-based segmentation propagation framework using locally affine registration -Application to automatic whole heart segmentation. *MICCAI* 2008

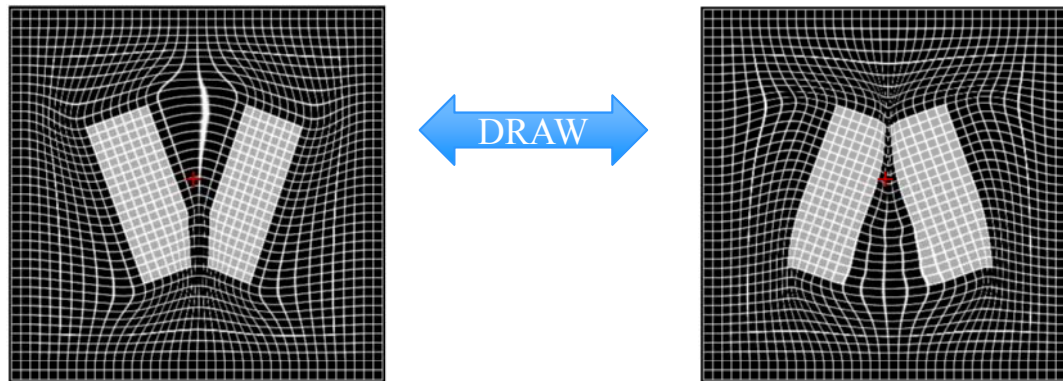
Zhuang, X., *et al.*: Free-Form Deformations Using Adaptive Control Point Status for Whole Heart MR Segmentation. *Functional Imaging and Modelling of the Heart* 2009

Zhuang, X., *et al.*: A Registration-Based Propagation Framework for Automatic Whole Heart Segmentation of Cardiac MRI. *IEEE Trans. Med. Imag.* 29 (9), 1612-1625, 2010.



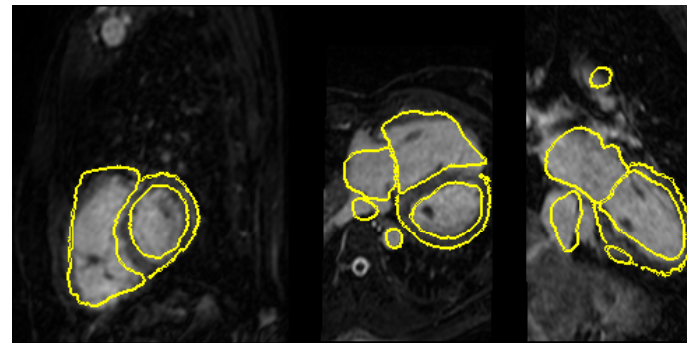
Shape from **an** atlas + LARM = model the variations for all cardiac images with different shapes

- **DRAW**: compute inverse transformation using Dynamic Resampling And distance Weighting interpolation
 - Maximal error is subvoxel for inverting dense displacements
 - Fast computation (~1minute for 3D cardiac application)

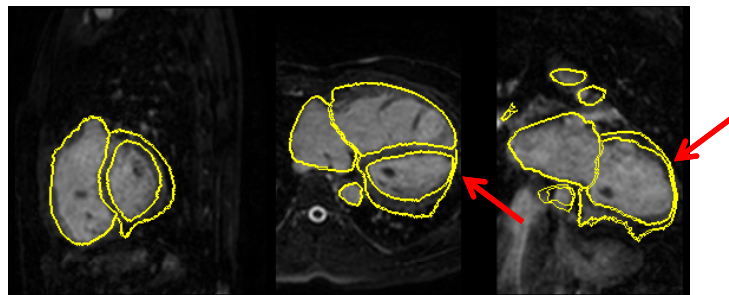


- **ACPS FFDs**: free-form deformation registration with adaptive control point status
 - To incorporate prior knowledge for nonrigid registration

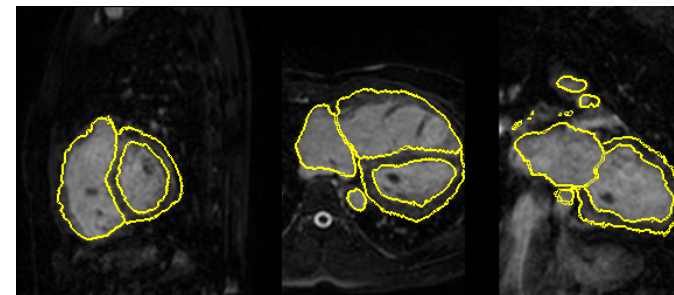
Good initialization by locally affine registration



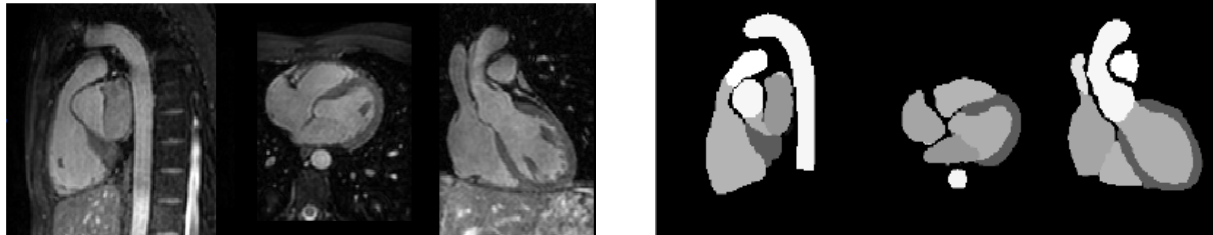
FFD registration propagation result



ACPS FFD registration propagation result

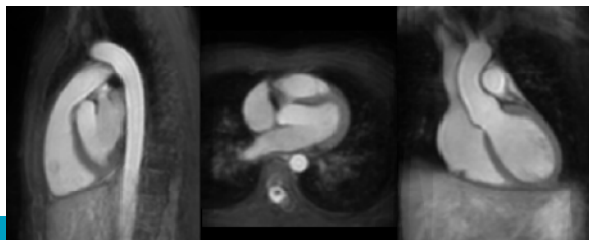


- Data:
 - 3D cardiac MRI
 - **A variety of pathologies and heart morphologies**
19 of 37 with confirmed pathologies (from 9 different pathologies)
 - Manually segmentation for each case



- Atlas:
 - One atlas intensity image and one label image
 - **No statistical information for shapes, nor intensity distributions**

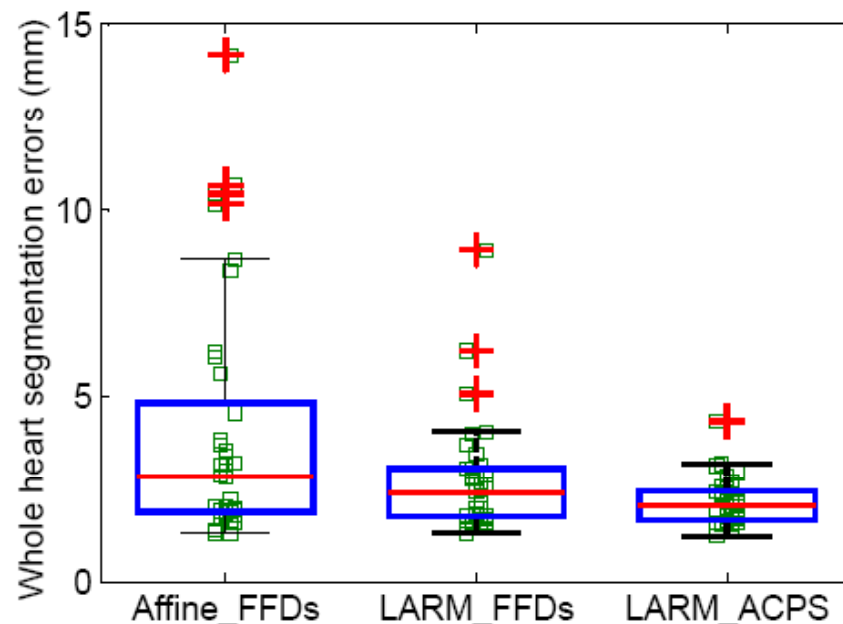
Atlas intensity image



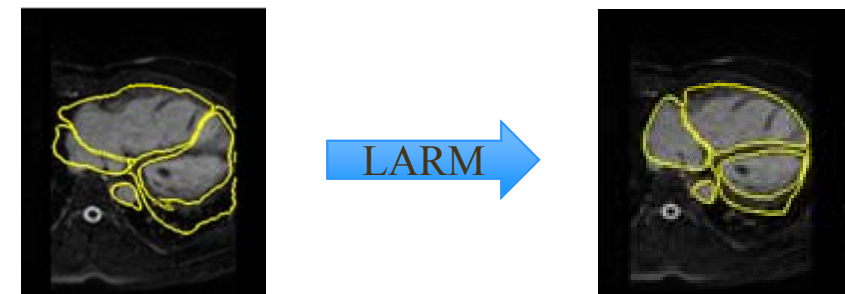
Atlas label image



- Propagation using alternative techniques
 - Affine_FFDs: global affine registration + traditional FFD registration
 - LARM_FFDs: global affine registration + LARM + traditional FFD registration
 - LARM_ACPS: global affine registration + LARM + ACPS FFD registration



Box-and-Whisker diagrams of the whole heart segmentation errors using the RMS surface-to-surface error measure, the errors of the 37 cases using the three different segmentation frameworks.

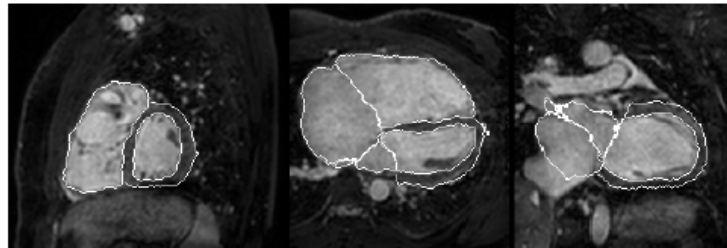


(a)

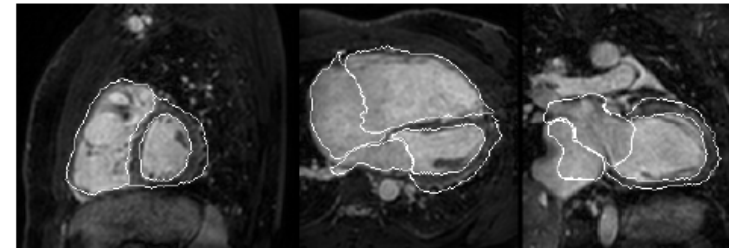


(b)

- Three worst cases



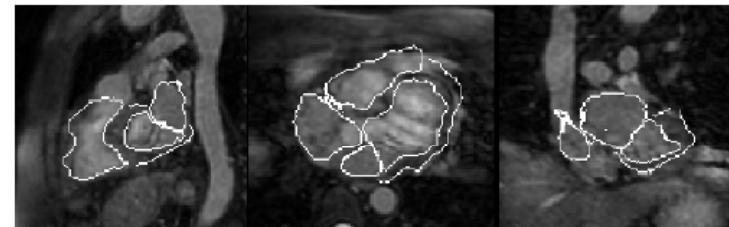
Subject-1, gold standard segmentation



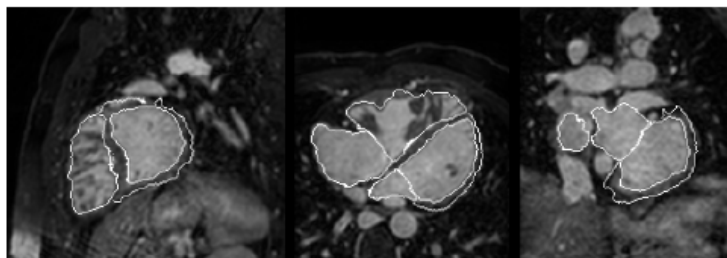
Subject-1, *LARM_ACPS* segmentation



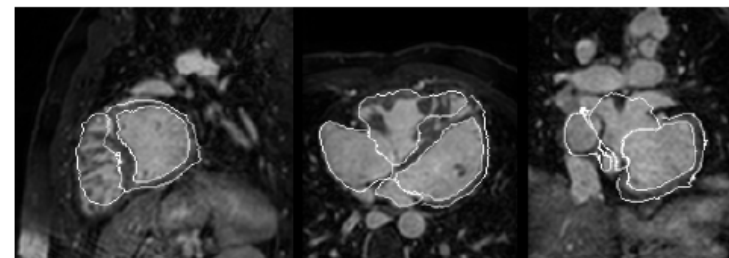
Subject-116, gold standard segmentation



Subject-116, *LARM_ACPS* segmentation



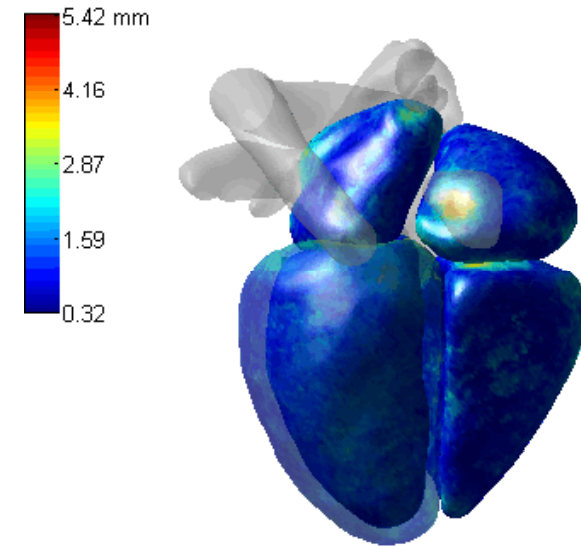
Subject-9, gold standard segmentation



Subject-9, *LARM_ACPS* segmentation

The three worst cases by the three segmentation methods. Subject-1 is the worst case of the Affine FFDs, subject-116 is the worst case of LARM FFDs, and subject-9 is the worst case of LARM ACPS. Images are displayed with delineated contour superimposing on the MR images, in sagittal, transverse, and coronal views. Subject-1 and subject-9 are pathological cases while subject-116 is a healthy case.

- Quantitative results
 - Color map of surface-to-surface errors of the whole heart segmentation
(The 37 cases were mapped to a common space to compute the average error of them)
 - Visualize performance
The big errors mainly distributed to the area of connections between substructures

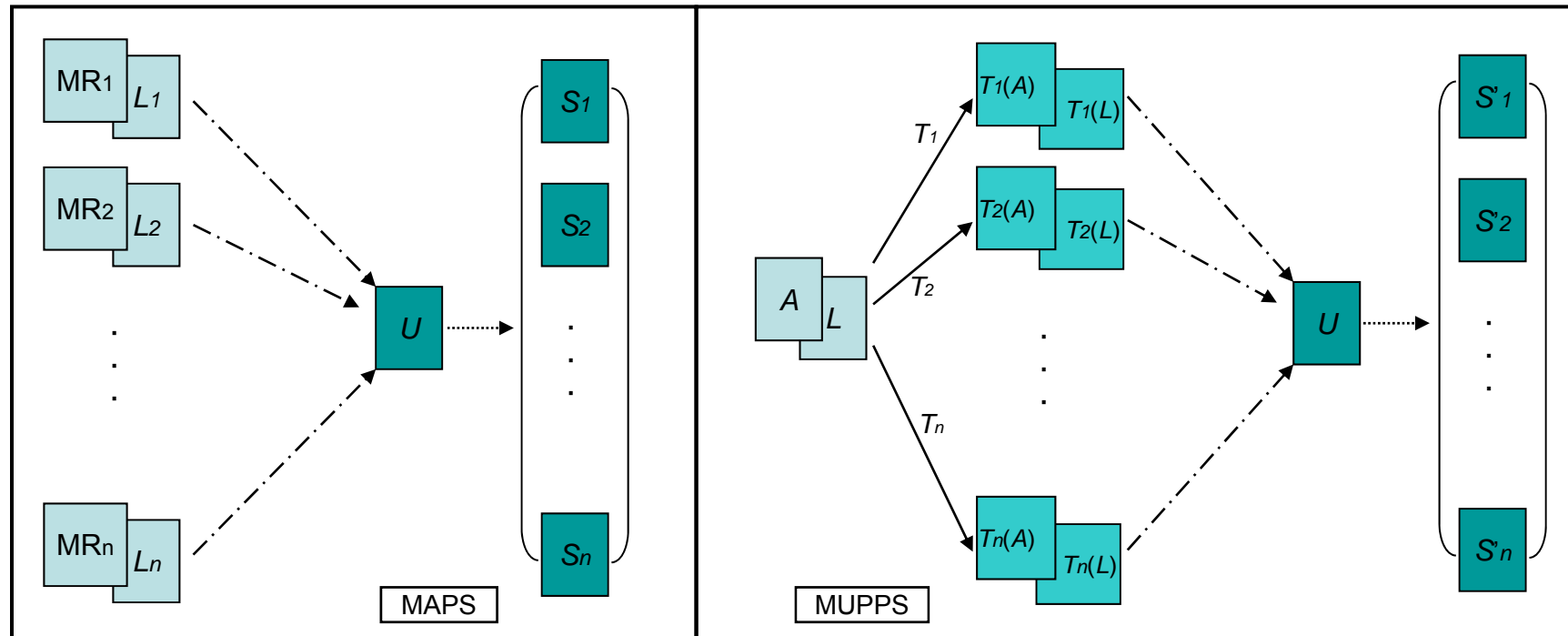


- Quantitative results for all local region, using different error measures

(error in mm) Structures	Affine_FFDs	LARM_FFDs	LARM_ACPS in different measures (ranges are of unit mm)					
	ϵ_{rms} [max]	ϵ_{rms} [max]	ϵ_{rms} [max]	ϵ_{mean}	ϵ_{std}	0 – 2	2 – 5	> 5
Left Ventricle	3.79 ± 4.38[19.6]	1.89 ± 1.10[7.12]	1.47 ± 0.32 [2.38]	1.06	1.02	82.9%	16.5%	0.6%
Left Atrium	3.26 ± 2.25[11.5]	2.81 ± 1.65[9.28]	2.38 ± 1.14 [7.33]	1.69	1.68	70.2%	23.5%	6.4%
Right Ventricle	3.23 ± 1.79[7.50]	2.75 ± 1.51[8.57]	2.13 ± 0.70 [4.05]	1.50	1.51	72.2%	24.1%	3.7%
Right Atrium	3.06 ± 1.74[9.44]	2.51 ± 1.20[7.05]	2.22 ± 0.75 [5.74]	1.51	1.62	73.0%	22.5%	4.5%
Epicardium	4.78 ± 4.88[20.4]	2.88 ± 2.12[12.9]	2.32 ± 0.82 [5.43]	1.69	1.60	68.6%	25.7%	5.6%
Whole Heart	3.96 ± 3.23[14.2]	2.71 ± 1.50[8.93]	2.14 ± 0.63 [4.31]	1.47	1.55	73.6%	22.5%	3.9%

Structures	Dice[min]	Overlap[min]	Diff(%) [max]	P-value (CI mL)	Pearson <i>R</i>
Left Ventricle	0.92 ± 0.02[0.87]	0.85 ± 0.04[0.78]	6.5 ± 4.9[19.0]	0.028 (0.5,7.5)	0.942
Left Atrium	0.81 ± 0.10[0.47]	0.69 ± 0.12[0.30]	14.1 ± 12.0[48.4]	0.667 (-2.7,4.2)	0.861
Right Ventricle	0.87 ± 0.04[0.77]	0.77 ± 0.06[0.63]	7.5 ± 4.9[19.7]	0.048 (0.1,12.3)	0.977
Right Atrium	0.84 ± 0.05[0.71]	0.73 ± 0.07[0.55]	9.0 ± 7.2[28.7]	0.217 (-6.8,1.6)	0.965
Myocardium	0.77 ± 0.06[0.52]	0.63 ± 0.07[0.35]	8.6 ± 6.9[26.7]	0.940 (-4.7,5.1)	0.892
All substructures	0.84 ± 0.08[0.47]	0.73 ± 0.10[0.30]	10.0 ± 9.6[48.4]	0.097 (-0.3,3.7)	0.974

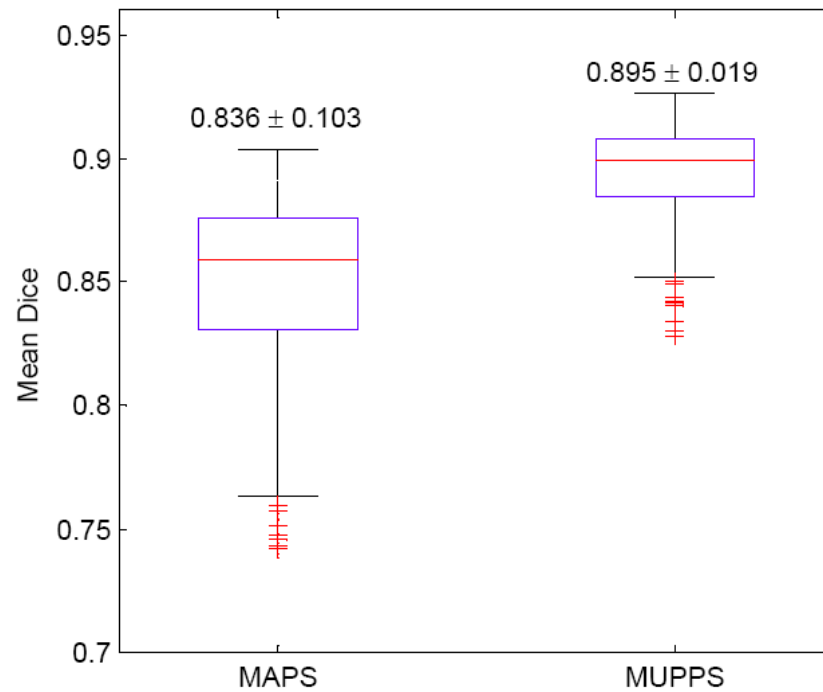
- Whole heart segmentation
 - Method
 - Localisation: global affine registration
 - **Initialisation**: Locally Affine Registration Method
 - Hierarchy scheme to increase the degree of freedom
 - Dynamic Resampling And distance Weighting interpolation
 - **Refine**: free form deformation registration with adaptive control point status
 - Validation: robust against a variety of pathologies
- Extension: to further improve accuracy
 - Multiple classification strategy
 - Refine with voxel-based classification techniques for accurate myocardium segmentation
 - Combining images from multiple MRI sequences for simultaneous segmentation



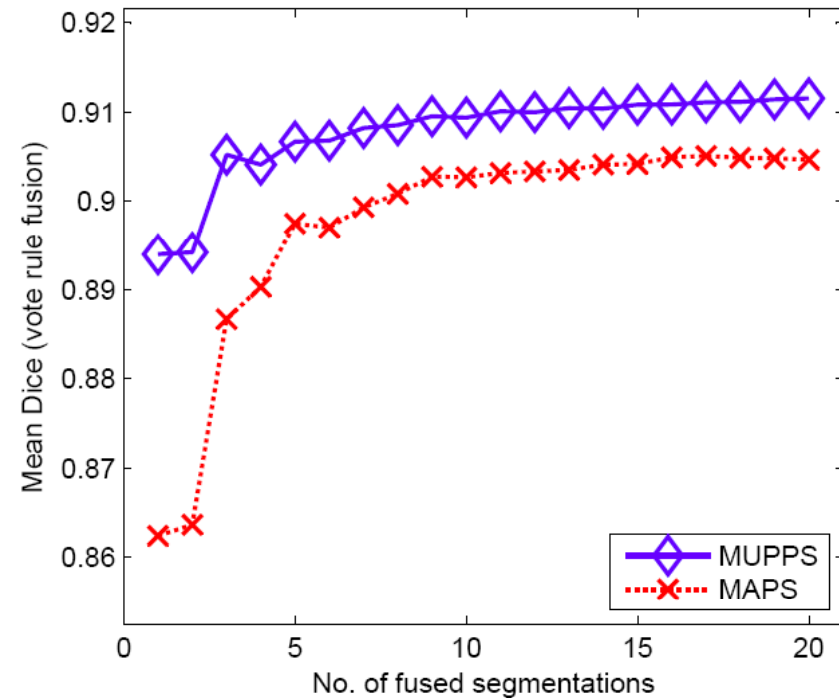
MAPS: multi-atlas propagation and segmentation

MUPPS: multiple path propagation and segmentation

- U: unseen images
- A: atlas intensity image
- {MR}: cardiac MR images
- {L}: segmentation labels
- {T}: deformation which initializes the propagation path
- {S}: segmentation propagation results

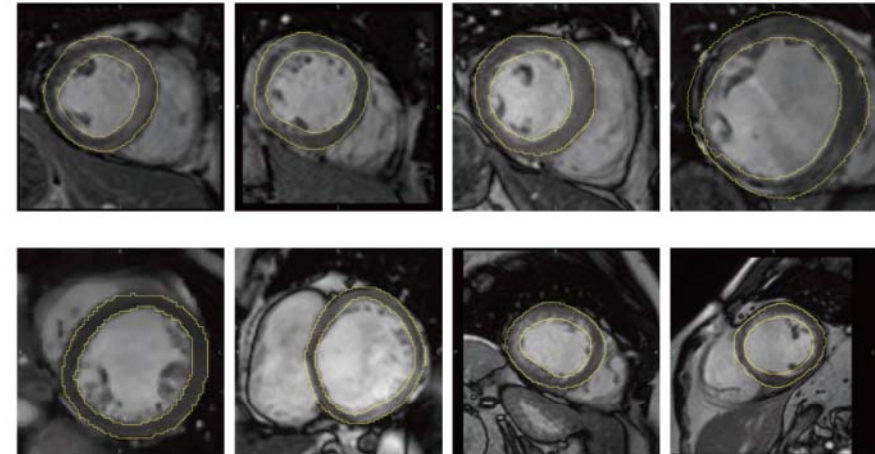
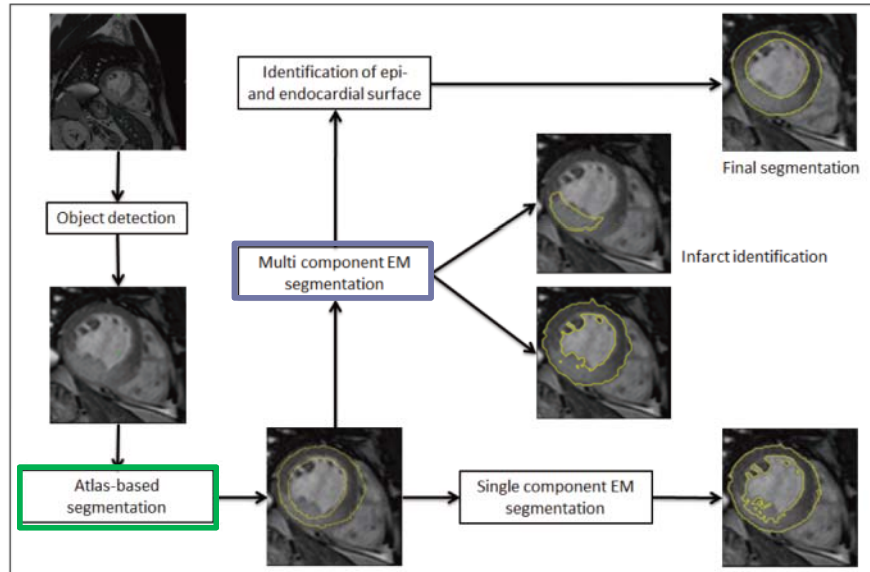


Box-and-Whisker diagram of the Dice scores using MAPS and MUPPS.



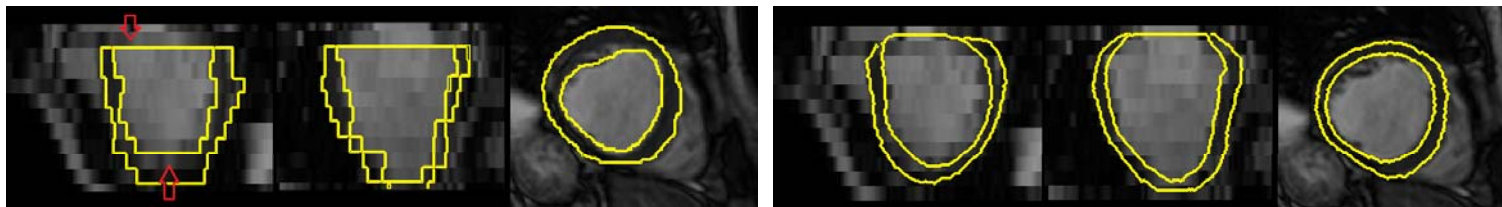
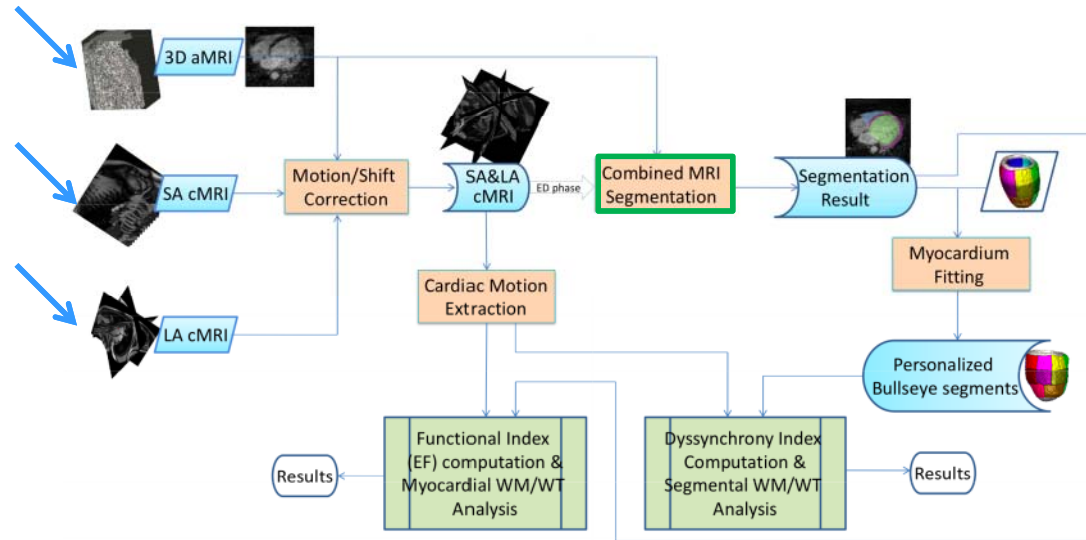
Dice scores from the VOTE fusion results of them

- Combine atlas propagation and voxel-based classification



Randomly selected results of eight different patients (from 90 subjects)

- Segmentation – extracting regions; Registration – motion tracking



Segmentation from single sequence (short-axis) Segmentation from multi-sequence MRIs
Red arrows point out the main difference by the two segmentation methods.